

Optical properties of ternary and quaternary IV–VI semiconductor layers on (100) BaF₂ substrates

Patrick J. McCann^{a)} and Lin Li

School of Electrical Engineering and Laboratory for Electronic Properties of Materials, University of Oklahoma, Norman, Oklahoma 73019

John E. Furneaux

Department of Physics and Astronomy and Laboratory for Electronic Properties of Materials, University of Oklahoma, Norman, Oklahoma 73019

Robert Wright

Department of Materials Science and Engineering, University of California, Los Angeles, California 90024 and The Aerospace Corporation, Los Angeles, California 90009

(Received 11 October 1994; accepted for publication 2 January 1995)

Fourier transform infrared (FTIR) absorption spectra and photoluminescence (PL) spectra for PbSe_{0.78}Te_{0.22} and Pb_{0.95}Sn_{0.05}Se_{0.80}Te_{0.20} layers grown by liquid phase epitaxy on (100) BaF₂ substrates are reported. FTIR absorption edges varied from 213 to 275 meV (between 4 and 300 K) for the ternary alloy and from 118 to 200 meV (between 10 and 300 K) for the quaternary alloy. PL energies were 174 meV at 5 keV for the ternary alloy and 100 meV at 7.1 K for the quaternary alloy. The differences between the low temperature FTIR absorption edge energies and the PL energies are attributed to the Burstein–Moss effect. © 1995 American Institute of Physics.

The band gap energies of IV–VI semiconductors, which have direct gaps at the *L* point in the Brillouin zone, range from 0 to 0.4 eV. Because the band gaps depend strongly on temperature, lasers made from these materials exhibit large tuning ranges,¹ making them uniquely suited for high resolution molecular spectroscopy applications.² Efforts to improve IV–VI semiconductor laser performance (i.e., mode stability and maximum operating temperatures), however, have been hindered by the high cost and limited availability of IV–VI semiconductor substrates. Recent development, though, of a new liquid phase epitaxy (LPE) process for growth of narrow band gap IV–VI semiconductor alloys on low cost BaF₂ substrates³ offers new opportunities to advance IV–VI semiconductor materials and device technologies. In this letter, we present infrared absorption and photoluminescence (PL) spectroscopic data for two IV–VI semiconductor alloys, PbSe_{0.78}Te_{0.22} and Pb_{0.95}Sn_{0.05}Se_{0.80}Te_{0.20}, grown by LPE on (100) BaF₂ substrates. These materials can comprise the cladding and active layers, respectively, of a double heterostructure laser. We show that such a laser will have a tuning range from 10.3 μ m at 77 K to 6.4 μ m at 275 K.

Ternary and quaternary IV–VI semiconductor epitaxial layers were grown on polished 4 mm×4 mm×380 μ m thick (100) BaF₂ substrates cut from ingots purchased from Bicorn, Inc., Solon, OH. The growth solution compositions were Pb_{0.97}(Se_{0.40}Te_{0.60})_{0.03} and (Pb_{0.95}Sn_{0.05})_{0.965}(Se_{0.46}Te_{0.54})_{0.035} with liquidus temperatures of 618 and 642 °C, respectively. Growth within the 610–660 °C temperature range is necessary in order to obtain continuous epitaxial layers owing to a temperature dependent substrate surface reaction,⁴ which catalyzes nucleation and thus promotes two-dimensional layer growth on BaF₂.⁵ The compositions

of the grown layers, obtained from x-ray diffraction lattice parameters and Vegard's Law, were PbSe_{0.78}Te_{0.22} for the ternary layer and Pb_{0.95}Sn_{0.05}Se_{0.80}Te_{0.20} for the quaternary layer. Uniform liquid-to-solid segregation between the group IV components was assumed for the quaternary layer. This assumption is valid based upon Auger electron spectroscopy (AES) compositional analysis of IV–VI semiconductor quaternary alloys.⁶ The ternary layer is lattice matched with the BaF₂ substrate (*a*₀=6.200 Å) while the quaternary layer (*a*₀=6.185 Å) has a lattice parameter mismatch of 0.25%.

Infrared absorption measurements were performed with a BioRad model FTS-60A Fourier transform infrared (FTIR) spectrometer using a variable temperature sample chamber equipped with KRS-5 windows. A Hg_{1-x}Cd_xTe detector with a cutoff wavelength of 14.3 μ m (87 meV) was used for all measurements. A sample placement geometry involving transmission through the substrate was allowed since the BaF₂ substrate is transparent to infrared radiation up to about 13 μ m (95 meV). PL measurements were performed with a specially designed long-wavelength spectrometer. The samples, mounted in a liquid-helium-cooled cryostat, were illuminated with the 514 nm line of an argon laser. Sample placement geometry involved transmission of epilayer generated photoluminescence through the BaF₂ substrate. This light, collected with a ZnSe lens, was passed through a set of circular variable filters (Optical Coating Laboratories, Inc.) spanning the 2.5–14.1 μ m spectral range and then focused with a second ZnSe lens on an arsenic-doped silicon-blocked impurity-band infrared detector with a 1–28 μ m spectral range.⁷

Figure 1 is a set of FTIR spectra showing absorbed light as a function of photon energy for a PbSe_{0.78}Te_{0.22} layer at various temperatures. The absorption edge energies decrease at a rate of 0.46 meV/K as the temperature is lowered from 300 to 100 K, though further decrease from 100 to 4 K is not

^{a)}Electronic mail: mccann@mailhost.ecn.uoknor.edu

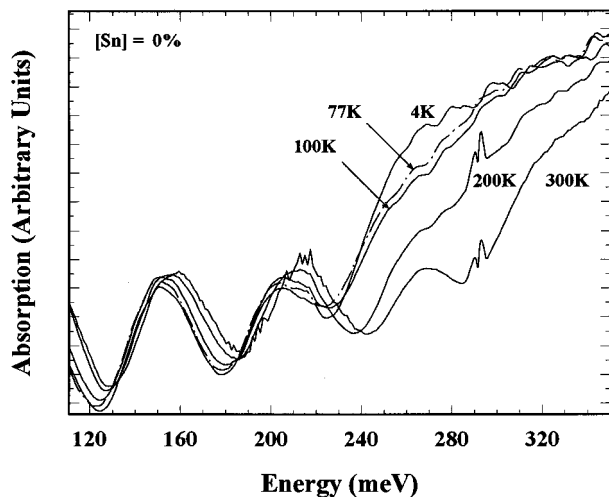


FIG. 1. FTIR absorption spectra obtained at various temperatures for a $\text{PbSe}_{0.78}\text{Te}_{0.22}$ layer grown by LPE on a (100) BaF_2 substrate. The broad absorption peaks at low energies are Fabry-Pérot interference fringes. Absorption peaks near 290 meV for the 300 and 200 K spectra are due to residual CO_2 in the spectrometer.

significant. The absorption peaks near 290 meV for the 300 and 200 K spectra are the *P* and *R* branches of the 2350 cm^{-1} ν_3 vibrational mode of CO_2 , and the small absorption peaks between 180 and 230 meV for the 300 K spectrum are associated with the $1450\text{--}1850\text{ cm}^{-1}$ H_2O absorption band. These peaks, which can be used to calibrate the spectra, are not evident at lower temperatures as the spectrometer was sufficiently purged during these measurements. Strong Fabry-Pérot interference fringes are also apparent at energies below the absorption edges. Epitaxial layer thickness was calculated from this fringe spacing using the equation $t = \lambda_1 \lambda_2 (m_1 - m_2) / 2(n_1 \lambda_2 - n_2 \lambda_1)$, where λ_1 and λ_2 are the wavelengths at the fringe maxima (or minima), m_1 and m_2 are integers corresponding to the orders of the fringes, and n_1 and n_2 are the refractive indices of the $\text{PbSe}_{0.78}\text{Te}_{0.22}$ alloy at the two different wavelengths. Using linearly extrapolated refractive index values calculated from published PbSe and PbTe data,⁸ an epilayer thickness of 2.18 μm is obtained. Figure 2 shows absorption spectra at various temperatures for the quaternary alloy. Compared to the ternary alloy, the absorption edges are shifted to lower energies. Fabry-Pérot interference fringes are also clearly apparent in the spectra and, using extrapolated refractive indices from published $\text{Pb}_{0.95}\text{Sn}_{0.05}\text{Se}$ and $\text{Pb}_{0.95}\text{Sn}_{0.05}\text{Te}$ data,⁸ their spacing yields a calculated epilayer thickness of 2.24 μm . These thicknesses are in good agreement with physically measured thicknesses of LPE-grown layers having similar growth times of about 5 min.³

PL spectra for the ternary and quaternary layers are shown in Fig. 3. The sample temperatures during the measurements were 5 and 7.1 K and the Argon laser pump powers were 12 and 9.3 mW, respectively. The ternary layer exhibited strong luminescence with a peak intensity at 174 meV along with a weaker, more broad luminescence between 325 and 475 meV. The 174 meV peak energy in the ternary spectrum compares well with the 185 meV peak energy ob-

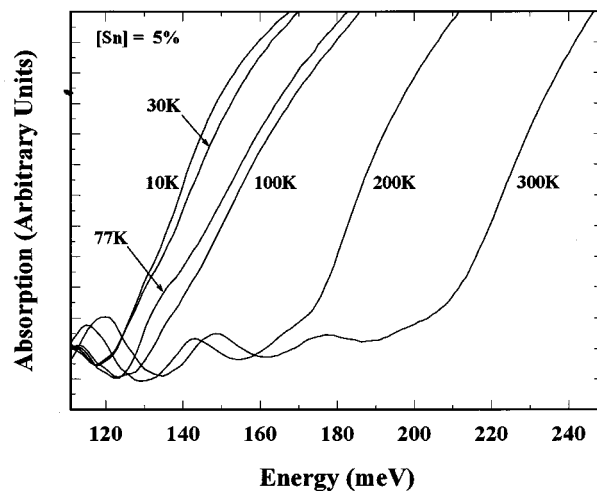


FIG. 2. FTIR absorption spectra obtained at various temperatures for a $\text{Pb}_{0.95}\text{Sn}_{0.05}\text{Se}_{0.80}\text{Te}_{0.20}$ layer grown by LPE on a (100) BaF_2 substrate. Fabry-Pérot interference fringes are also apparent in this sample. Note the shift to lower energies as compared to the ternary sample shown in Fig. 1.

served from a $\text{PbSe}_{0.80}\text{Te}_{0.20}$ layer at 77 K grown by hot wall epitaxy (HWE) on (111) BaF_2 .⁹ These peaks are clearly associated with direct interband transitions, the 11 meV difference due primarily to the band gap dependence on temperature. The higher energy peak in the ternary spectrum may be due to transitions associated with group VI vacancy defect levels in the conduction band. Our data suggest that these levels are approximately 200 meV above the bottom of the conduction band. The authors of Ref. 9 also observed weak higher energy PL peaks in their HWE samples, though the energy difference (at 77 K) was only 50 meV. The quaternary layer exhibited strong luminescence with a peak intensity at 100 meV, and, unlike the ternary sample, exhibited no other detectable luminescence.

Figure 4 summarizes the FTIR and PL data where the

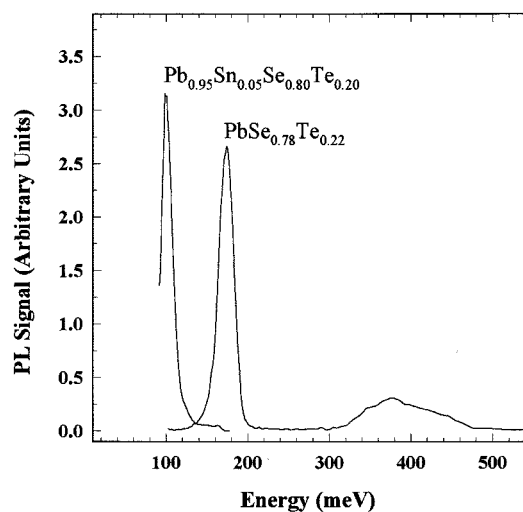


FIG. 3. PL spectra for $\text{PbSe}_{0.78}\text{Te}_{0.22}$ and $\text{Pb}_{0.95}\text{Sn}_{0.05}\text{Se}_{0.80}\text{Te}_{0.20}$ layers grown by LPE on (100) BaF_2 . The full width half-maximum are 21.8 and 16.0 meV, respectively. The broad peak between 325 and 475 meV may be associated with recombination from native (chalcogen vacancy) defect levels.

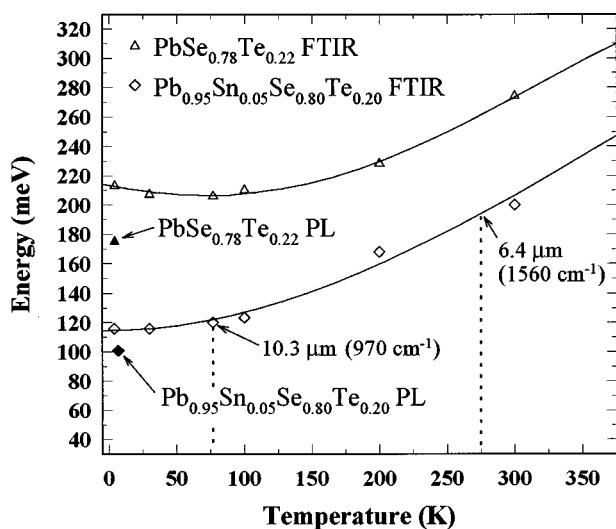


FIG. 4. FTIR absorption edge and PL energies vs temperature for undoped $\text{PbSe}_{0.78}\text{Te}_{0.22}$ and $\text{Pb}_{0.95}\text{Sn}_{0.05}\text{Se}_{0.80}\text{Te}_{0.20}$ layers grown by LPE. Differences between the PL and FTIR absorption energies at low temperature are believed to be due to the Burstein–Moss effect (Ref. 14). Corresponding wavelengths and wave numbers at 77 and 275 K are indicated.

FTIR absorption edge energies were obtained from the intersection of the square of the absorption slope with the lowest measured absorption between the interference fringes. This method, which assumes a parabolic band structure, has previously been used to obtain the band gaps of IV–VI semiconductor compounds.¹⁰ FTIR absorption edge energy dependence on temperature above 100 K for the ternary alloy is similar to the band gap dependence on temperature for $\text{PbSe}_{0.80}\text{Te}_{0.20}$ alloys grown by HWE based upon photovoltaic,¹¹ PL,⁹ and optical absorption¹² studies. At low temperatures, however, the FTIR absorption edge energies stop decreasing with temperature, whereas the PL peak energy at 5 K is near the line extrapolated from the high temperature FTIR data and is in good agreement with the $\text{PbSe}_{0.80}\text{Te}_{0.20}$ HWE data. A similar discrepancy exists for the quaternary alloy except that the difference between the FTIR absorption edge energy and the PL energy at 7 K is about 18 meV instead of about 40 meV for the ternary alloy.

Because of the large electron concentration in these LPE-grown semiconductors,¹³ differences between the PL and FTIR absorption edge energies at low temperatures can be assigned to the Burstein–Moss effect.¹⁴ If phonon-assisted interband transitions are neglected (likely at low temperatures) and symmetric valence and conduction bands are assumed (known to be the case for IV–VI semiconductors) the position of the Fermi energy in the conduction band can be estimated by dividing the amount of shift by a factor of 2. This yields values of 20 meV for the ternary alloy and 9 meV for the quaternary alloy. The smaller energy shift for the quaternary layer may be due to a smaller electron concentration in this material. Addition of tin in $\text{Pb}_{1-x}\text{Sn}_x\text{Se}$ and $\text{Pb}_{1-x}\text{Sn}_x\text{Te}$ alloys is known to shift the solid solubility limit of group VI vacancies toward the pseudobinary stoichiometry composition and at high enough concentrations converts the material to *p* type.¹⁵ It is thus likely that the quaternary

$\text{Pb}_{0.95}\text{Sn}_{0.05}\text{Se}_{0.80}\text{Te}_{0.20}$ alloy has a somewhat smaller electron concentration than the ternary alloy.

The data presented here can be used to design double heterostructure lasers in which the quaternary alloy is the active region. Our data show that $\text{PbSe}_{0.78}\text{Te}_{0.22}$ cladding layers provide conduction and valence band edge discontinuities, assuming equal offsets, of approximately 40 meV over a wide range of temperatures. Such a laser is expected to have a tuning range from 10.3 μm (970 cm^{-1}) to 6.4 μm (1560 cm^{-1}) when heated from 77 to 275 K as indicated in Fig. 4. Although the $\text{Pb}_{0.95}\text{Sn}_{0.05}\text{Se}_{0.80}\text{Te}_{0.20}$ quaternary alloy studied here is not lattice matched with BaF_2 or the $\text{PbSe}_{0.78}\text{Te}_{0.22}$ ternary alloy and is grown at a higher than usual temperature, its optical properties should be similar to the lattice-matched $\text{Pb}_{0.95}\text{Sn}_{0.05}\text{Se}_{0.76}\text{Te}_{0.24}$ alloy, which has recently been grown by LPE.¹⁶ The properties of quaternary active layers grown on $\text{PbSe}_{0.78}\text{Te}_{0.22}$ should, in fact, be better since growth is possible at much lower temperatures (there is no need for an epitaxy-enabling substrate surface reaction⁵). It is expected that the Burstein–Moss shift in such layers will decrease since lower growth temperatures will reduce the native electron concentration.

In summary, FTIR absorption spectra and PL spectra for ternary $\text{PbSe}_{0.78}\text{Te}_{0.22}$ and quaternary $\text{Pb}_{0.95}\text{Sn}_{0.05}\text{Se}_{0.80}\text{Te}_{0.20}$ layers grown by LPE on (100) BaF_2 substrates were presented. The FTIR data above 100 K show that the band gaps of these alloys increase with temperature at a rate of 0.46 meV/K, in good agreement with band gap measurements of other IV–VI semiconductor alloys. Observed Fabry–Pérot interference spacing also allowed accurate calculation of the epilayer thicknesses. Strong PL with low argon laser pump intensities were obtained from both layers indicating that these materials are suitable for laser fabrication. Differences between the low temperature FTIR absorption edge energies and the PL peak energies are believed to be result of the Burstein–Moss effect. This effect is less pronounced in the quaternary alloy.

- ¹J. N. Walpole, A. R. Calawa, T. C. Harman, and S. H. Groves, *Appl. Phys. Lett.* **28**, 552 (1976).
- ²R. S. Eng, J. F. Butler, and K. J. Linden, *Opt. Eng.* **19**, 945 (1980).
- ³P. J. McCann and C. G. Fonstad, *Thin Solid Films* **227**, 185 (1993).
- ⁴P. J. McCann and C. G. Fonstad, *J. Electron. Mater.* **20**, 915 (1991).
- ⁵P. J. McCann, *Mater. Res. Soc. Symp. Proc.* **221**, 289 (1991).
- ⁶P. J. McCann, J. Fuchs, Z. Feit, and C. G. Fonstad, *J. Appl. Phys.* **62**, 2994 (1987).
- ⁷M. D. Petroff, M. G. Stapelbroek, and W. A. Kleinhan, *Appl. Phys. Lett.* **51**, 406 (1987).
- ⁸P. K. Cheo, *Handbook of Solid State Lasers* (Marcel Dekker, New York, 1989).
- ⁹M. V. Valeiko, I. I. Zasavitskii, V. L. Kuznetsov, A. V. Kurganskii, and B. N. Matsonashvili, *Sov. Phys. Semicond.* **19**, 388 (1985).
- ¹⁰W. W. Scanlon, *J. Phys. Chem. Solids* **8**, 423 (1959).
- ¹¹A. Jedrzejczak, D. Guillot, and G. Martinez, *Phys. Rev. B* **17**, 829 (1978).
- ¹²L. I. Bytenskii, V. I. Kaidanov, R. B. Melnik, S. A. Nemov, and Yu. I. Ravich, *Sov. Phys. Semicond.* **14**, 40 (1980).
- ¹³P. J. McCann, S. Aanegola, and J. E. Furneaux, *Appl. Phys. Lett.* **65**, 2185 (1994).
- ¹⁴E. Burstein, *Phys. Rev.* **93**, 632 (1954); T. S. Moss, *Proc. Phys. Soc. B* **67**, 775 (1954).
- ¹⁵T. C. Harman, *J. Nonmetals* **1**, 183 (1973).
- ¹⁶P. J. McCann and D. Zhong, *J. Appl. Phys.* **75**, 1145 (1994).